Full-field microimaging with 8 keV X-rays achieves a spatial resolutions better than 20 nm

Tsung-Yu Chen,[1] Yu-Tung Chen,[1] Cheng-Liang Wang,[1] Ivan M. Kempson,[1] Wah-Keat Lee,[2] Yong S. Chu,[3,7] Y. Hwu,[1,4,5,*] G. Margaritondo[6]

[1]*Institute of Physics, Academia Sinica, Taipei 115, Taiwan*
[2]*Advanced Photon Source, Argonne National Laboratory, Argonne, IL 60439, USA*
[3]*National Synchrotron Light Source II, Brookhaven National Laboratory, Upton, NY 11973, USA*
[4]*Department of Engineering and System Science, National Tsing Hua University, Hsinchu 300, Taiwan*
[5]*Advanced Optoelectronic Technology Center, National Cheng Kung University, Tainan 701, Taiwan*
[6]*Ecole Polytechnique Fédérale de Lausanne (EPFL), CH-1015 Lausanne, Switzerland*
[7]*ychu@bnl.gov*
**phhwu@sinica.edu.tw &*

Abstract: Fresnel zone plates (450 nm thick Au, 25 nm outermost zone width) used as objective lenses in a full field transmission reached a spatial resolution better than 20 nm and 1.5% efficiency with 8 keV photons. Zernike phase contrast was also realized without compromising the resolution. These are very significant achievements in the rapid progress of high-aspect-ratio zone plate fabrication by combined electron beam lithography and electrodeposition.

OCIS codes: (110.7440) Imaging systems: X-ray imaging; (180.7460) Microscopy: X-ray microscopy.

References and links

1. G. Margaritondo, Y. Hwu, and J. H. Je, "Synchrotron light in medical and materials science radiology," Riv. Nuovo Cim. **27**, 1–40 (2004).
2. X. Cai, H. H. Chen, C. L. Wang, S. T. Chen, S. F. Lai, C. C. Chien, Y. Y. Chen, I. M. Kempson, Y. Hwu, C. S. Yang, and G. Margaritondo, "Imaging the cellular uptake of tiopronin-modified gold nanoparticles," Anal. Bioanal. Chem. **401**(3), 809–816 (2011).
3. P. C. Hsu, Y. S. Chu, J. Yi, C. L. Wang, S. R. Wu, Y. Hwu, and G. Margaritondo, "Dynamical growth behavior of copper clusters during electrodeposition," Appl. Phys. Lett. **97**(3), 033101 (2010).
4. H. H. Chen, C. C. Chien, C. Petibois, C. L. Wang, Y. S. Chu, S. F. Lai, T. E. Hua, Y. Y. Chen, X. Cai, I. M. Kempson, Y. Hwu, and G. Margaritondo, "Quantitative analysis of nanoparticle internalization in mammalian cells by high resolution X-ray microscopy," J. Nanobiotechnology **9**(1), 14 (2011).
5. F. K. Huang, W. C. Chen, S. F. Lai, C. J. Liu, C. L. Wang, C. H. Wang, H. H. Chen, T. E. Hua, Y. Y. Cheng, M. K. Wu, Y. Hwu, C. S. Yang, and G. Margaritondo, "Enhancement of irradiation effects on cancer cells by cross-linked dextran-coated iron oxide (CLIO) nanoparticles," Phys. Med. Biol. **55**(2), 469–482 (2010).
6. Y. T. Chen, T. N. Lo, C. W. Chiu, J. Y. Wang, C. L. Wang, C. J. Liu, S. R. Wu, S. T. Jeng, C. C. Yang, J. Shiue, C. H. Chen, Y. Hwu, G. C. Yin, H. M. Lin, J. H. Je, and G. Margaritondo, "Fabrication of high-aspect-ratio Fresnel zone plates by e-beam lithography and electroplating," J. Synchrotron Radiat. **15**(2), 170–175 (2008).
7. D. Attwood, *Soft X-Rays and Extreme Ultraviolet Radiation: Principles and Applications* (Cambridge University Press, Cambridge, 1999).
8. G. C. Yin, Y. F. Song, M. T. Tang, F. R. Chen, K. S. Liang, F. W. Duewer, M. Feser, W. Yun, and H. P. D. Shieh, "30 nm resolution x-ray imaging at 8 keV using third order diffraction of a zone plate lens objective in a transmission microscope," Appl. Phys. Lett. **89**(22), 221122 (2006).
9. S. Rehbein, S. Heim, P. Guttmann, S. Werner, and G. Schneider, "Ultrahigh-resolution soft-X-ray microscopy with zone plates in high orders of diffraction," Phys. Rev. Lett. **103**(11), 110801 (2009).
10. J. Yi, Y. S. Chu, Y. T. Chen, T. Y. Chen, Y. Hwu, and G. Margaritondo, "High-resolution hard-X-ray microscopy using second-order zone plate diffraction," J. Phys. D Appl. Phys. **44**(23), 232001 (2011).
11. W. Chao, B. D. Harteneck, J. A. Liddle, E. H. Anderson, and D. T. Attwood, "Soft X-ray microscopy at a spatial resolution better than 15 nm," Nature **435**(7046), 1210–1213 (2005).
12. W. Chao, J. Kim, S. Rekawa, P. Fischer, and E. H. Anderson, "Demonstration of 12 nm resolution Fresnel zone plate lens based soft X-ray microscopy," Opt. Express **17**(20), 17669–17677 (2009).
13. Y. T. Chen, T. N. Lo, Y. S. Chu, J. Yi, C. J. Liu, J. Y. Wang, C. L. Wang, C. W. Chiu, T. E. Hua, Y. Hwu, Q. Shen, G. C. Yin, K. S. Liang, H. M. Lin, J. H. Je, and G. Margaritondo, "Full-field hard x-ray microscopy below 30 nm: a challenging nanofabrication achievement," Nanotechnology **19**(39), 395302 (2008).

#148769 - $15.00 USD Received 13 Jun 2011; revised 19 Aug 2011; accepted 24 Aug 2011; published 27 Sep 2011

14. Y. T. Chen, T. Y. Chen, J. Yi, Y. S. Chu, W. K. Lee, C. L. Wang, I. M. Kempson, Y. Hwu, V. Gajdosik, and G. Margaritondo, "Hard x-ray Zernike microscopy reaches 30 nm resolution," Opt. Lett. **36**(7), 1269–1271 (2011).
15. C. C. Chien, C. H. Wang, C. L. Wang, E. R. Li, K. H. Lee, Y. Hwu, C. Y. Lin, S. J. Chang, C. S. Yang, C. Petibois, and G. Margaritondo, "Synchrotron microangiography studies of angiogenesis in mice with microemulsions and gold nanoparticles," Anal. Bioanal. Chem. **397**(6), 2109–2116 (2010).
16. T. N. Lo, Y. T. Chen, C. W. Chiu, C. J. Liu, S. R. Wu, I. K. Lin, C. I. Su, W. D. Chang, Y. Hwu, B. Y. Shew, C. C. Chiang, J. H. Je, and G. Margaritondo, "E-beam lithography and electrodeposition fabrication of thick nanostructured devices," J. Phys. D Appl. Phys. **40**(10), 3172–3176 (2007).
17. S. S. Sarkar, H. H. Solak, J. Raabe, C. David, and J. F. van der Veen, "Fabrication of Fresnel zone plates with 25 nm zone width using extreme ultraviolet holography," Microelectron. Eng. **87**(5-8), 854–858 (2010).
18. R. Divan, D. C. Mancini, N. Moldovan, B. Lai, L. Assoufid, Q. Leonard, and F. Cerrina, "Progress in the fabrication of high-aspect-ratio zone plates by soft X-ray lithography," SPIE **4783**, 82–91 (2002).
19. M. Altissimo, F. Romanato, L. Vaccari, L. Businaro, D. Cojoc, B. Kaulich, S. Cabrini, and E. D. Fabrizio, "X-ray lithography fabrication of a zone plate for X-rays in the range from 15 to 30 keV," Microelectron. Eng. **61–62**(1-3), 173–177 (2002).
20. L. Liu, G. Liu, Y. Xiong, J. Chen, W. Li, and Y. Tian, "Fabrication of X-ray imaging zone plates by e-beam and X-ray lithography," Microsyst. Technol. **16**(8-9), 1315–1321 (2010).
21. Y. F. Song, C. H. Chang, C. Y. Liu, S. H. Chang, U. S. Jeng, Y. H. Lai, D. G. Liu, S. C. Chung, K. L. Tsang, G. C. Yin, J. F. Lee, H. S. Sheu, M. T. Tang, C. S. Hwang, Y. K. Hwu, and K. S. Liang, "X-ray beamlines for structural studies at the NSRRC superconducting wavelength shifter," J. Synchrotron Radiat. **14**(4), 320–325 (2007).
22. Q. Shen, W.-K. Lee, K. Fezzaa, Y. S. Chu, F. De Carlo, P. Jemian, J. Ilavsky, M. Erdmann, and G. G. Long, "Dedicated full-field X-ray imaging beamline at Advanced Photon Source," Nucl. Instrum. Methods A **582**(1), 77–79 (2007).
23. Y. S. Chu, J. M. Yi, F. De Carlo, Q. Shen, W.-K. Lee, H. J. Wu, C. L. Wang, J. Y. Wang, C. J. Liu, C. H. Wang, S. R. Wu, C. C. Chien, Y. Hwu, A. Tkachuk, W. Yun, M. Feser, K. S. Liang, C. S. Yang, J. H. Je, and G. Margaritondo, "Hard-x-ray microscopy with Fresnel zone plates reaches 40 nm Rayleigh resolution," Appl. Phys. Lett. **92**(10), 103119 (2008).
24. S. Vogt, G. Schneider, A. Steuernagel, J. Lucchesi, E. Schulze, D. Rudolph, and G. Schmahl, "X-ray microscopic studies of the drosophila dosage compensation complex," J. Struct. Biol. **132**(2), 123–132 (2000).
25. J. Yi, Y. S. Chu, Y. T. Chen, T. Y. Chen, Y. Hwu, and G. Margaritondo, "High-resolution hard-X-ray microscopy using second-order zone plate diffraction," J. Phys. D Appl. Phys. **44**(23), 232001 (2011).

The spatial resolution of hard-X-ray microscopy is steadily advancing in the nanoscale range. This is important since such a technique offers complementary advantages with respect to visible and electron microscopy: the diffraction limit does not impede nanoscale imaging and the sample requirements are rather relaxed. In fact, with hard-X-rays, thick (several hundreds μm) samples can be imaged in a flexible and controllable environment [1–5].

Here we report a significant achievement that is likely to impact, in particular, the applications to biomedical research and materials science. Full-field hard-X-ray microscopy surpassed the 20 nm resolution level with good contrast (thanks to a Zernike ring). This result could be obtained after solving some challenging technical problems [6].

Full-field imaging, a preferred mode for many applications, is preferentially implemented with Fresnel zone plates (ZP) because of their high efficiency and low aberrations [7]. The full-field ZP resolution is ideally $\alpha\Delta r/m$, where Δr is the outmost zone width, m the diffraction order and α a factor determined by the optical aberrations and by the coherence level of the radiation [7]. Higher diffraction orders thus provide higher resolution [8–10]. However, the price is a drastic signal reduction that prevents fast imaging and can lead to radiation damage by prolonged exposure.

Improving the resolution therefore requires decreasing Δr. This must be done while keeping the ZP thickness large enough to provide good efficiency in spite of the low hard-X-ray absorption. The corresponding high aspect ratio is a significant nanofabrication challenge. As a consequence, the <20 nm resolution reported for soft X-rays [11,12] could not be matched so far for hard-X-rays [13,14]. This is regrettable since the higher penetration of hard-X-rays facilitates imaging of thicker and/or denser samples [15], and offers other advantages.

Our present tests do demonstrate a hard-X-ray ZP spatial resolution better than 20 nm. Figure 1 schematically shows the experimental system used for such tests. The resolution was

#148769 - $15.00 USD Received 13 Jun 2011; revised 19 Aug 2011; accepted 24 Aug 2011; published 27 Sep 2011

assessed by imaging a star test pattern and by a power spectrum analysis of the micrographs. The tests were performed both for absorption contrast and for Zernike phase contrast.

The main problems in fabricating high-aspect-ratio [16] ZPs are rigidity and strength. We obtained ZPs meeting these requirements by sequentially using electron beam lithography and electrodeposition [16]. The results appear better than those of alternate methods including UV holography [17] and X-ray lithography [18–20].

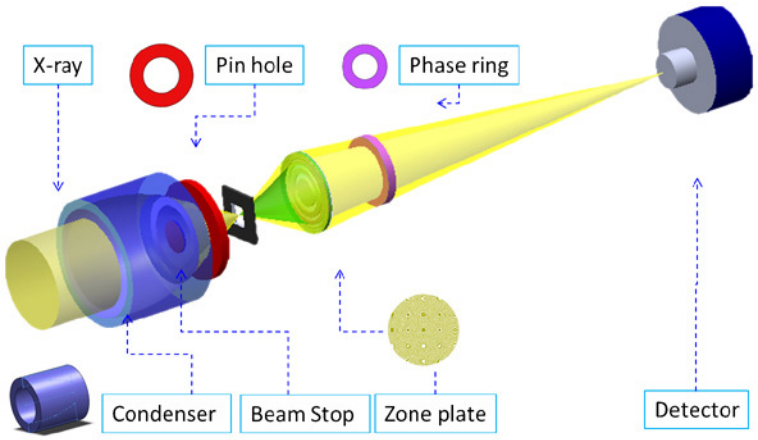

Fig. 1. Schematics layout of our full-field hard-X-ray transmission microscope using a ZP as an objective lens.

The structure of our 25 nm outermost zone ZPs consisted of a gold pattern over a 1 μm thick silicon nitride membrane. The membrane was obtained with low pressure chemical vapor deposition (LPCVD) on a research-grade Si(100) wafer. The backside was etched by KOH to remove silicon until only the membrane was left. Then, we deposited a 5 nm Cr buffer layer and a 12 nm gold layer. Photoresist (polymethyl methacrylate, PMMA A6) was used to spin-coat the metal-covered membrane and then thermally cured at 170 C for 15 min.

Electron beam writing (with an Elionix ELS-7000 system operating at 100 keV and 10 pA) then produced a specially designed ZP pattern. This was based on a broken-line geometry [16] to avoid the collapse of the developed photoresists due to the high aspect ratio. The pattern shape was empirically optimized by trial-and-error adjustments of the electron beam writing duty cycle to reduce line distortion effects. The electron beam dose was also empirically optimized: this was a critical step that could not be automatically implemented. In the specific case of the ZP of 25 nm outermost zone we used an electron beam current of 25 pA and an average dosage of 1100 μC/cm^2; other zone width required an adjustment: the dosage was decreased by 50 μC/cm^2 for every 5 nm reduction of the width.

The photoresist pattern was developed with a 7:3 mixture of IPA (isopropanol) and water for 30 s to completely remove the electron-beam-exposed parts [16]. The final metal nanostructure was obtained by gold electrodeposition in the open trenches of the resist pattern. Details of the electrodeposition procedure, similar to LECD (localized electrochemical deposition), can be found in Ref. 16.

This method produced the ZPs used in this study with the following key features of the gold nanostructures. The ZP diameter was 50 μm, the width of the outermost zone was 25 nm and the metal nanostructure as thick as 500 nm in the best case. Therefore, the aspect ratio reaches 500/25 = 20. The fine structure of the 25 nm ZP is evidenced by its Moiré pattern in SEM micrographs of Fig. 2.

The ZPs were first checked at the 01BL beamline [21] of National Synchrotron Radiation Research Center (NSRRC, Taiwan). Final tests were then performed on the full-field imaging transmission X-ray microscope at the 32-ID beamline [22] of the Advanced Photon Source,

#148769 - $15.00 USD Received 13 Jun 2011; revised 19 Aug 2011; accepted 24 Aug 2011; published 27 Sep 2011

Argonne National Laboratory (APS). A Si(111) double-crystal monochromator provided there an X-ray beam of 8 keV with a flux of $2x10^{11}$ photon/sec. The high brightness allowed imaging with exposures as short as 50 ms [23].

The microscope system included an initial diffuser to homogenize the intensity of the incoming X-ray beam, which was then focused on the sample plane by a capillary condenser system optimized for 8 keV. The ZP was used to create the transmitted X-ray image in a scintillator crystal, which could be captured with a CCD camera. A pinhole and a central beamstop completely block out the unfocused beam from the condenser.

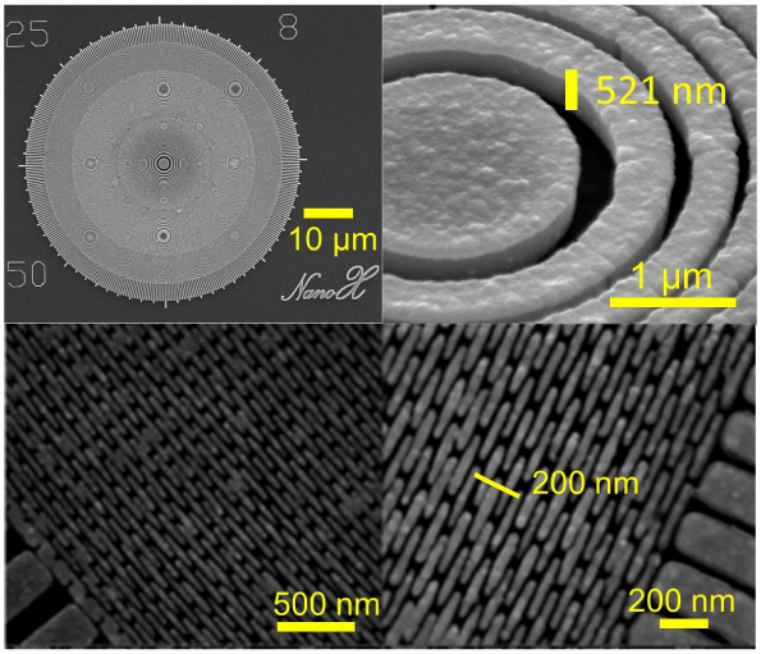

Fig. 2. SEM image of a zone plate with Δr = 25 nm and a thickness of 500nm.

The resolution can be evaluated from the start test pattern images (Fig. 3a) by power spectrum analysis (Fig. 3b) as previously described [13,24]. In short, the image was multiplied by a gradient function to remove edge artifacts before a two-dimensional Fourier transform. Integration over the resulting frequency space image yielded the power spectrum. Large image features contributed to the low frequency part of the spectrum whereas at higher frequencies the finer structures prevailed before being overwhelmed by the background noise, and become unrecognizable. Test patterns imaged by different ZPs with 45, 40, 30, 25 nm outermost zones are shown in Fig. 3a. The power spectra show the progressive improvement of the minimum detectable feature size above the noise, reflected by the shift of the cutoff towards high frequencies. The 25 nm ZP achieved the best resolution, <20 nm.

Spatial resolution is not the only performance criterion: for many applications, notably in the life sciences, image contrast is also significant. The contrast can be augmented by the Zernike phase method. However, one must check that this does not sacrifice the resolution. We tested this point for the ZP with 25 nm outermost zone width using a matched phase ring and performing the same analysis as in Fig. 3. Figure 4a shows two images obtained with and without a Zernike phase ring at the back focal plane of the ZP. The phase ring was fabricated by the similar Au electrodeposition procedure on SiN membrane. The dimension of the ring is 11.2 µm in diameter, 1.5 µm in width and 2.6 µm thick. Typical power spectra like those of Fig. 4b reveal here a ~16 nm resolution for both cases. This value is consistent with the

#148769 - $15.00 USD Received 13 Jun 2011; revised 19 Aug 2011; accepted 24 Aug 2011; published 27 Sep 2011

theoretical resolution based on partially coherent illumination, 0.6-0.8 times the outermost zone width [12].

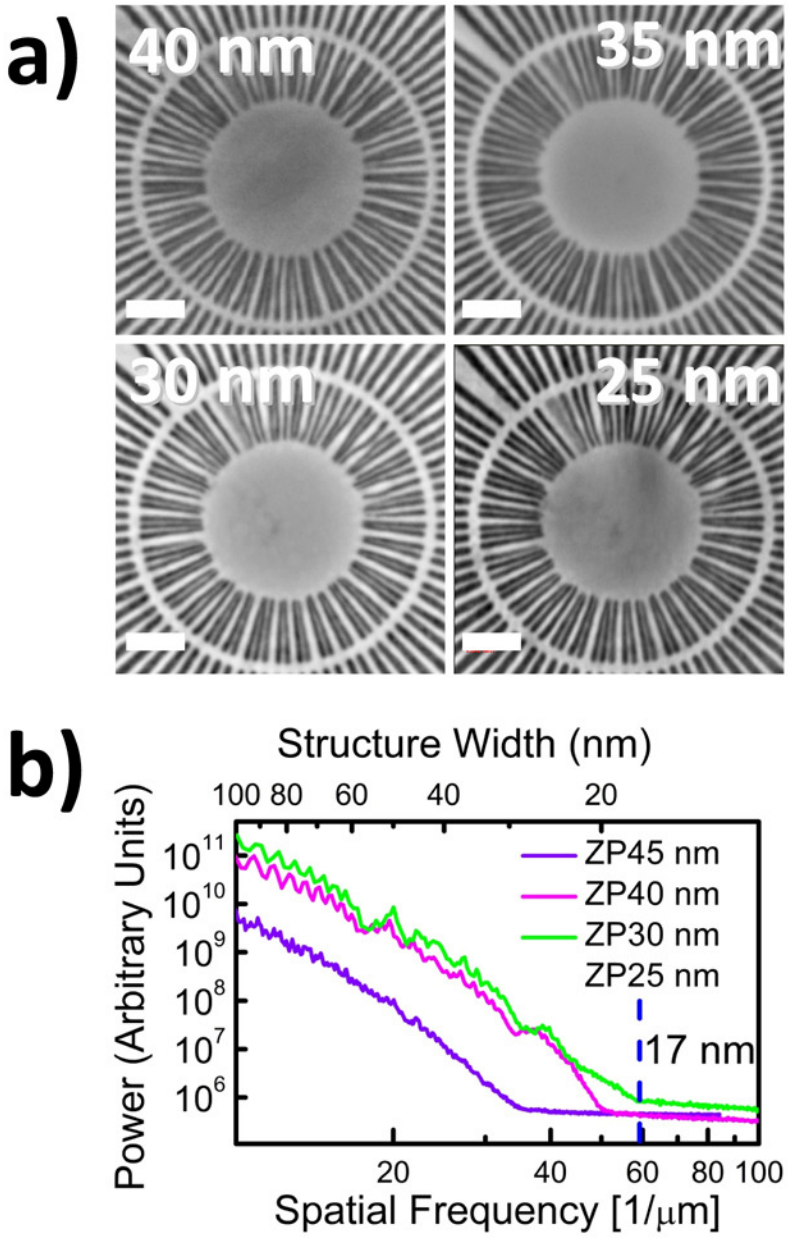

Fig. 3. (a) TXM images of a test pattern with innermost Au features of 30 nm pitch, taken using one of our best ZPs (25 nm outermost zone width) as well as with other ZPs with larger (45, 40, 30) outermost zone widths. Bars: 2 μm. (b) The power spectrum analysis of these images showsthe highest spatial frequency corresponding to the minimum-size features detectable above the noise, <20 nm for the 25 nm ZP.

The efficiency is another important ZP performance parameter. We evaluated it by taking the integrated-intensity ratio of the first-order diffracted beam and the zero-order direct beam, both of which could be projected on the CCD with the 2X objective. Note that the deviation of the duty cycle from unity, seen in Fig. 2 for zones with width < 40 nm, attributes to the

#148769 - $15.00 USD Received 13 Jun 2011; revised 19 Aug 2011; accepted 24 Aug 2011; published 27 Sep 2011

reduction of efficiency: the theoretical efficiency of 500 nm-thick Au ZP with the mark to space ratio of 1:1 at 8keV is 8% (6.6% for 450 nm thick) [25]. Values of 1-1.5% measured for the tested ZPs were thus coherent with the theoretical predictions. Together with the excellent resolution levels and the Zernike-enhanced contrast, this performance makes our best ZPs very valuable for biomedical and materials sciences investigations.

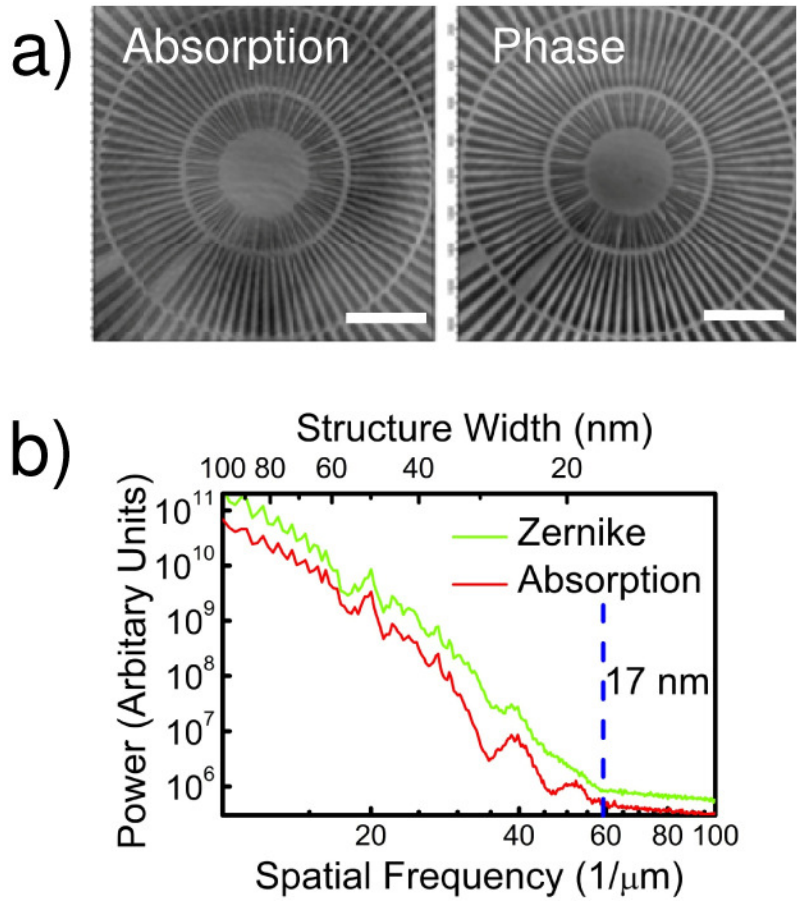

Fig. 4. (a) Images of the same test pattern as in Fig. 3 with (right) and without (left) Zernike phase contrast using the 25 nm ZP. The brightness difference between bright and dark areas indicates a contrast ratio ~12%. Bars: 5 μm. (b) A power spectrum analysis confirms a resolution <20 nm.

Acknowledgements

This research was supported by National Science and Technology for Nanoscience and Nanotechnology, the Academia Sinica, the National Synchrotron Radiation Research Center (Taiwan), the Fonds National Suisse pour la Recherche Scientifique, the EPFL, the CIBM, and the Brookhaven Science Associates, LLC under Contract No. DE-AC02-98CH10886. Use of the Advance Photon Source is supported by the U. S. Department of Energy, Office of Science, Office of Basic Energy Sciences, under Contract No. DE-AC02-06CH11357.

#148769 - $15.00 USD Received 13 Jun 2011; revised 19 Aug 2011; accepted 24 Aug 2011; published 27 Sep 2011